

Neuromuscular System of the Flexible Arm of the Octopus: Physiological Characterization

Henry Matzner, Yoram Gutfreund and Binyamin Hochner
J Neurophysiol 83:1315-1328, 2000.

You might find this additional info useful...

This article cites 36 articles, 20 of which can be accessed free at:

<http://jn.physiology.org/content/83/3/1315.full.html#ref-list-1>

This article has been cited by 10 other HighWire hosted articles, the first 5 are:

Kinematics of Soft-bodied, Legged Locomotion in *Manduca sexta* Larvae

Barry Trimmer and Jonathan Issberner

Biol Bull 2007; 212 (2): 130-142.

[\[Abstract\]](#) [\[Full Text\]](#) [\[PDF\]](#)

Patterns of Motor Activity in the Isolated Nerve Cord of the Octopus Arm

Yoram Gutfreund, Henry Matzner, Tamar Flash and Binyamin Hochner

Biol Bull 2006; 211 (3): 212-222.

[\[Abstract\]](#) [\[Full Text\]](#) [\[PDF\]](#)

Locomotion by *Abdopus aculeatus* (Cephalopoda: Octopodidae): walking the line between primary and secondary defenses

Christine L. Huffard

J Exp Biol, October 1, 2006; 209 (19): 3697-3707.

[\[Abstract\]](#) [\[Full Text\]](#) [\[PDF\]](#)

Dynamic Model of the Octopus Arm. I. Biomechanics of the Octopus Reaching Movement

Yoram Yekutieli, Roni Sagiv-Zohar, Ranit Aharonov, Yaakov Engel, Binyamin Hochner and Tamar Flash

J Neurophysiol, August 1, 2005; 94 (2): 1443-1458.

[\[Abstract\]](#) [\[Full Text\]](#) [\[PDF\]](#)

Dynamic Model of the Octopus Arm. II. Control of Reaching Movements

Yoram Yekutieli, Roni Sagiv-Zohar, Binyamin Hochner and Tamar Flash

J Neurophysiol, August 1, 2005; 94 (2): 1459-1468.

[\[Abstract\]](#) [\[Full Text\]](#) [\[PDF\]](#)

Updated information and services including high resolution figures, can be found at:

<http://jn.physiology.org/content/83/3/1315.full.html>

Additional material and information about *Journal of Neurophysiology* can be found at:

<http://www.the-aps.org/publications/jn>

This information is current as of October 11, 2011.

Neuromuscular System of the Flexible Arm of the Octopus: Physiological Characterization

HENRY MATZNER, YORAM GUTFREUND, AND BINYAMIN HOCHNER

Department of Neurobiology and Center for Neuronal Computation, Institute of Life Sciences, Hebrew University, Jerusalem 91904, Israel

Matzner, Henry, Yoram Gutfreund, and Binyamin Hochner. Neuromuscular system of the flexible arm of the octopus: physiological characterization. *J. Neurophysiol.* 83: 1315–1328, 2000. The octopus arm is an outstanding example of an efficient boneless and highly flexible appendage. We have begun characterizing the neuromuscular system of the octopus arm in both innervated muscle preparations and dissociated muscle cells. Functionally antagonistic longitudinal and transverse muscle fibers showed no differences in membrane properties and mode of innervation. The muscle cells are excitable but have a broad range of linear membrane properties. They are electrotonically very compact so that localized synaptic inputs can control the membrane potential of the entire muscle cell. Three distinct excitatory neuronal inputs to each arm muscle cell were identified; their reversal potentials were extrapolated to be about -10 mV. These appear to be cholinergic as they are blocked by hexamethonium, D-tubocurarine, and atropine. Two inputs have low quantal amplitude (1–7 mV) and slow rise times (4–15 ms), whereas the third has a large size (5–25 mV) and fast rise time (2–4 ms). This large synaptic input is most likely due to exceptionally large quantal events. The probability of release is rather low, suggesting a stochastic activation of muscle cells. All inputs demonstrated a modest activity-dependent plasticity typical of fast neuromuscular systems. The pre- and postsynaptic properties suggest a rather direct relation between neuronal activity and muscle action. The lack of significant electrical coupling between muscle fibers and the indications for the small size of the motor units suggest that the neuromuscular system of the octopus arm has evolved to ensure a high level of precise localization in the neural control of arm function.

INTRODUCTION

This report is part of a comprehensive study of the octopus arm as a model system for motor control and biomechanical functions of flexible arms (Gutfreund et al. 1996, 1998). The octopus arm, like other cephalopod tentacles, vertebrate tongues, and the elephant trunk, lacks any form of rigid skeleton. In contrast to articulated appendages, the muscles in these structures supply skeletal support as well as generating movements. Because these structures are composed mainly of incompressible muscle tissue, Kier and Smith (1985) have termed them muscular hydrostats.

Apart from the specialized neuromuscular system of the chromatophors (Bone et al. 1995; Florey et al. 1985; Packard 1995), little is known about the physiology of cephalopod neuromuscular systems. Electromyographic recordings of muscle activity have provided some insights into the neuromuscu-

lar system of the muscular hydrostats comprising the mantle and fin of cephalopods (Gosline et al. 1983; Kier et al. 1989; Wilson 1960; for review, see Bone et al. 1995). Synaptic transmission first was investigated in these neuromuscular systems by Stockbridge and Stockbridge (1988), who showed that spontaneous synaptic activity consists of very large, presumably quantal, events and that the nerve-evoked release is very unsynchronized. However, because of technical limitations they were unable to address several important issues such as the pattern and mode of innervation, the postsynaptic integrative properties of the muscle cells, and the characteristics of transmitter release properties. Further characterization of such systems is needed to determine whether cephalopod muscular hydrostats have evolved unique neuromuscular mechanisms.

We show here that the neuromuscular system of the octopus arm has several features not found in other neuromuscular systems. The small, electrically compact and excitable muscle cells are innervated by three distinct cholinergic excitatory synaptic inputs. One of these inputs has an exceptionally large unitary size, and all showed a modest activity-dependent plasticity. Longitudinal and transverse muscle groups are composed of uniform neuromuscular units with rather simple integrative and transformational properties. These results demonstrate several neuromuscular features that may have evolved as an adaptive solution to the complex problem of motor control in flexible arms.

METHODS

Specimens of *Octopus vulgaris* were collected by local fishermen in the Mediterranean Sea or imported from the Stazione Zoologica, Naples, Italy. The octopuses were kept individually in aquaria of artificial seawater, which circulated through a closed system of biological filters. Aquaria were regulated to 17°C, 12 h light/dark cycle, and the octopuses were fed fish meat once a day. These conditions enabled us to keep the octopuses for ≤ 6 mo, during which they gained weight at what seemed to be a normal rate.

The animals were anesthetized in cold seawater containing 2% ethanol. A short segment, 1–3 cm long, was dissected from the middle of the arm and kept in artificial seawater (ASW) at $\sim 10^\circ\text{C}$. ASW composition was (in mM) 460 NaCl, 10 KCl, 55 MgCl₂, 11 CaCl₂, 10 glucose, and 10 HEPES, pH 7.6. The animal displayed normal behavior after the operation, and the amputated arm readily regenerated as in the natural environment.

Dissociated muscle cells

Dissociated muscle cells were prepared according to the method of Brezina et al. (1994). A small piece of arm muscle was taken from a

The costs of publication of this article were defrayed in part by the payment of page charges. The article must therefore be hereby marked "advertisement" in accordance with 18 U.S.C. Section 1734 solely to indicate this fact.

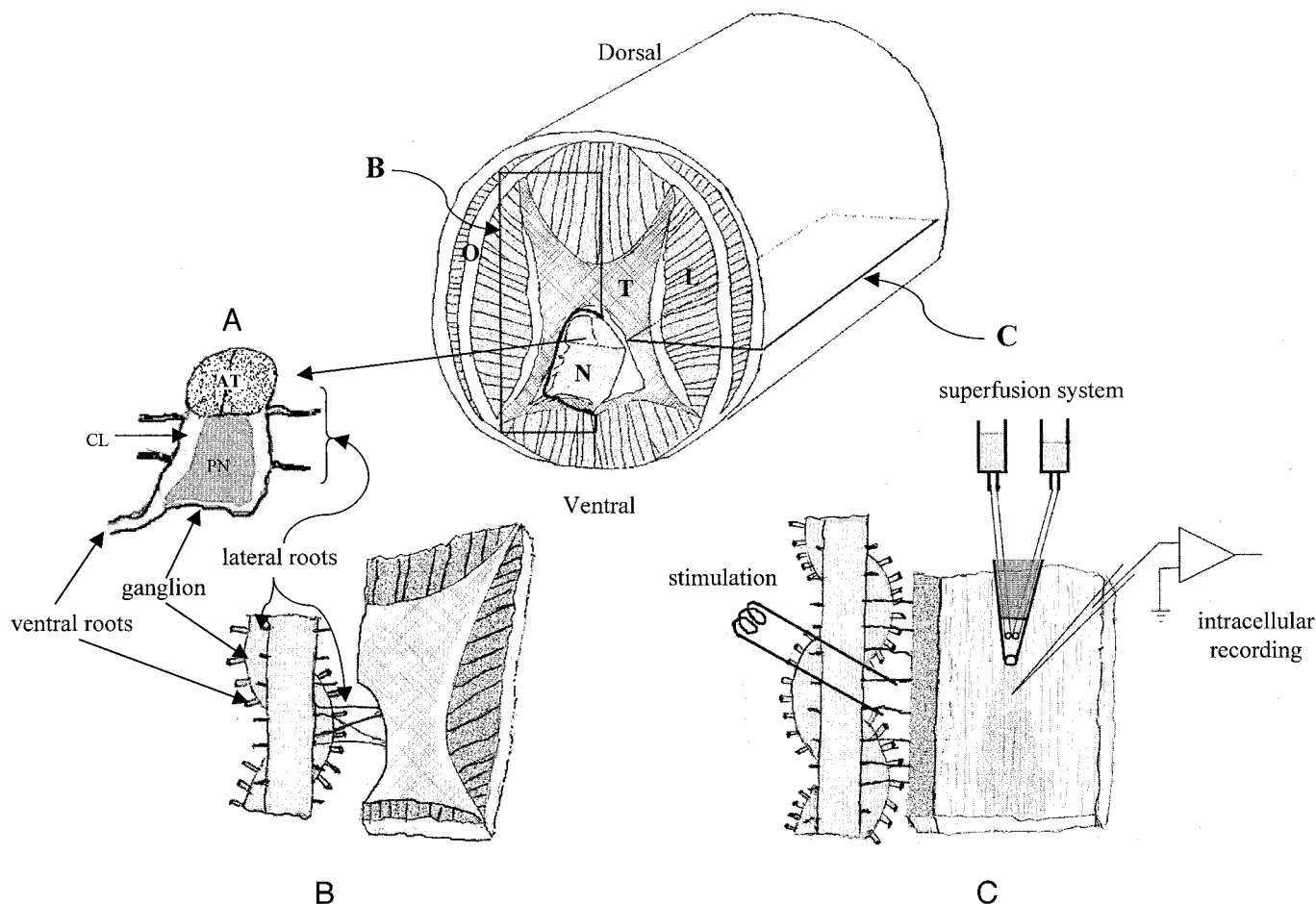


FIG. 1. Schematic description of the neuromuscular organization of the octopus arm and the 2 types of preparations used to study the transverse (*B*) and longitudinal (*C*) neuromuscular systems. (Areas where the muscle fibers are transversely sectioned are stippled; hatched areas show where muscle fibers are cut in a plane parallel to the longitudinal axis of the fibers, which are ~ 1 mm long.) *Top inset*: cross-section of the intrinsic musculature with suckers (on the ventral side) and subdermal muscles removed (the diameter of such a cross-section, taken from the middle of a typical arm 25 cm long, is ~ 8 mm). Muscle cells are organized in 3 orientations: longitudinal (L, stippled), transverse (T, cross-hatched), and oblique (O, clear). Dark lines that cross the longitudinal muscles represent trabeculae of transverse muscle fibers. Transverse muscles surround the axial nerve cord (N), which runs along the arm and contains ~ 300 ganglia. *A*: axial nerve cord is divided into a dorsally located axonal tract (AT), a ganglionic part with a layer of cell bodies in the periphery (CL), and an internal neuropil (PN). Nerve roots emerging from the ganglia innervate the suckers via the ventral roots and the intrinsic muscles via the lateral roots. *B*: arrangement of the transverse muscle preparation. Location and direction of sectioning is depicted in the *top inset* (marked B). Muscle strand is rotated 90° with respect to the axial nerve cord, which is viewed from above. Lateral nerve roots, which innervate the muscle strand, were left intact for stimulation. *C*: arrangement of longitudinal muscle preparation made by dissecting along the plane indicated C in the *top inset*. Lateral nerve roots were stimulated with bipolar electrodes. Area of recording was superfused by a system designed for rapid exchange of solution at the recording site (see METHODS).

designated area of the intrinsic musculature of the arm under microscopic control. The tissue was incubated at 25°C for 2–4 h in 0.2% collagenase (Sigma Type I) dissolved in Leibovitz L15 culture medium (Biological Industries, Bet Haemek, Israel), adjusted to the concentration of salts in the seawater. Rinsing with L15 terminated the enzymatic treatment. The tissue then was triturated manually until an appreciable concentration of dissociated cells could be detected in the supernatant. These cells were kept at 4°C for ≤ 4 days; their physiological properties did not appear to deteriorate during this period. For electrophysiological experiments, an aliquot of the cells was transferred to a plastic petri dish mounted on an inverted microscope. The cells settled on the bottom of the dish after a few minutes.

The electrical properties of the isolated muscle cell were investigated in the whole cell current-clamp mode, using the Axoclamp 2B (Axon Instruments). The patch pipettes were filled with the following internal solution (in mM): 465 K-gluconate, 2 MgCl_2 , 1 CaCl_2 , 10 K-EGTA, 5 Na_2ATP , 50 HEPES, buffered to pH 7.2 with KOH. In

several experiments, EGTA concentration was reduced to $10 \mu\text{M}$ to avoid major disturbance to the cell's buffering system while still chelating excess Ca^{2+} in the internal pipette solution.

Innervated muscle preparation

A small muscle strand of $\sim 10 \text{ mm}^2$ was dissected out in the planes shown in Fig. 1 together with three to six ganglia of the arm axial nervous system (a nerve cord length of ~ 6 – 12 mm). We concentrated on the longitudinal (Fig. 1C) and transverse (Fig. 1B) muscle fibers in the lateral and dorsal muscle groups (Fig. 1, *top inset*) (Graziadei 1971; Kier 1988). These are built of closely packed, obliquely striated muscle fibers typical of cephalopods (Bone et al. 1995; Kier 1985). These groups play a significant role in the generation of the arm extension and reaching movements being investigated in our laboratory (Gutfreund et al. 1996, 1998). The lateral nerve roots innervating the

muscle of interest (Graziadi 1971; Martoja and May 1956) were left intact for stimulation with bipolar Ag/AgCl electrodes (Fig. 1, A–C). The preparation was pinned down on a silicone elastomer (Sylgard)-coated dish and perfused with aerated artificial seawater at room temperature. Stimulating the nerve in fresh preparations frequently caused weak muscle twitches. These disappeared as the preparations equilibrated in the experimental bath. Intracellular recordings were made with sharp glass microelectrodes (25–40 M Ω when filled with 3 M K-acetate plus 0.1 M KCl) using the Axoclamp 2B in bridge mode. The results were stored on video recorder (Neuro-Corder, NeuroData) for later analysis.

The small size of the cells (Bone et al. 1995; unpublished results) made it difficult to obtain stable long-term recordings. We therefore constructed a superfusion system that allowed fast changes of solution at the recording site (see Fig. 1C). Briefly, the recording site was superfused continuously via a polyethylene tip drawn to a diameter of ~ 50 μ m and mounted on a micromanipulator. Hydrostatic pressure was used to drive four different solutions (only 2 are shown in Fig. 1C) through the polyethylene tubing (1.14 mm ID) right into the tip. The free space at the tip was rather small (~ 20 μ l), enabling exchange between the different solutions within a few seconds. Dye added to the solutions helped aim the stream at a desired location and control its flow. However, as recordings were made from cells in deeper tissue layers, the latencies of the effects of solution changes were variable, and the effective concentration of the drugs could not be precisely determined.

RESULTS

Passive and active membrane properties of the muscle fibers

The electrical properties of the muscle fibers were examined using whole cell recordings in enzymatically dissociated cells and in the innervated muscle preparation using sharp microelectrodes in a bridge mode (see METHODS).

Voltage responses to injection of long current pulses in dissociated cells are shown in Figs. 2, A and B, and 3, A and B. Responses in innervated muscle fibers are given in Figs. 2C and 3, C and D. The time constants and input resistances obtained in the whole cell configuration are much larger than those recorded intracellularly in the innervated muscles. In dissociated fibers, $R_{in} = 480 \pm 414$ M Ω (mean \pm SD; $n = 16$) and $\tau_m = 102 \pm 55$ ms ($n = 15$), but these only average 32.2 ± 12.8 M Ω ($n = 15$) and 23.8 ± 16.3 ms ($n = 14$) in the innervated muscle preparations. These differences are usually attributed to damage caused by the sharp microelectrodes (see Marty and Neher 1995).

The current-voltage relationship of both dissociated and innervated muscle cells shows a wide range of linear membrane properties. As shown in Fig. 2, B and C, this linearity exists in the range of membrane potential from about -100 to about -40 mV; the resting potential is -74 to -63 mV in both experimental conditions. Outward rectification starts at about -40 mV, which is close to the level of initiation of active currents (see following text). These findings indicate that the octopus muscle fibers serve as linear voltage integrators at a broad range of membrane potentials. (Note that fibers can contract at membrane potentials below the threshold of the regenerative potentials.)

The muscle cells can generate several types of regenerative responses that are activated at a relatively high membrane potential. Figure 3, A and B, illustrates the two main classes of regenerative activity detected in dissociated cells. We termed the cell in Fig. 3B a “spiky” cell because it responds to a

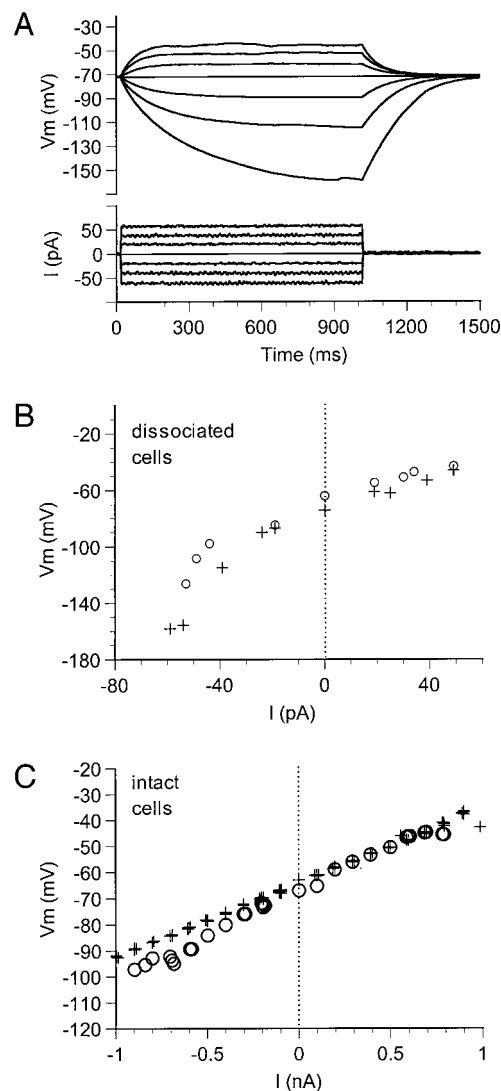


FIG. 2. Passive membrane properties of the muscle cells in dissociated and innervated muscle fiber preparations. A: typical passive membrane potential responses to 1-s current injections obtained in dissociated muscle fibers by the whole cell recording procedure. B: I - V relationship of 2 dissociated muscle cells based on results as in A. Voltage was measured at the end of the pulses. Note a linear relation range between -100 and -40 mV and a voltage-dependent increase in slope resistance at potentials below about -100 mV. C: 2 examples of the I - V relation of muscle cells obtained in innervated preparations. This demonstrates the broad linear range similar to that of dissociated cells (B), although with much lower input resistance.

long-lasting depolarization with a train of overshooting spikes. The threshold for spike initiation was about -30 mV, and spike frequency was related to current intensity. The cell in Fig. 3A showed a more complex behavior, which we term “oscillatory.” At around -45 mV (bottom trace), slow fluctuations in membrane potential appear during the current injection. At around -40 mV (Fig. 3A, \leftarrow), a slow regenerative response is initiated, followed by gradually increasing oscillations. These oscillations build up into a train of low-amplitude spikes. Some cells showed both patterns of behavior; after massive activation, the cell in Fig. 3B changed from spiky to oscillatory. Despite the large differences in the apparent passive membrane properties, similar types of cells showing either accelerating oscillations (Fig. 3C) or overshooting spikes (Fig.

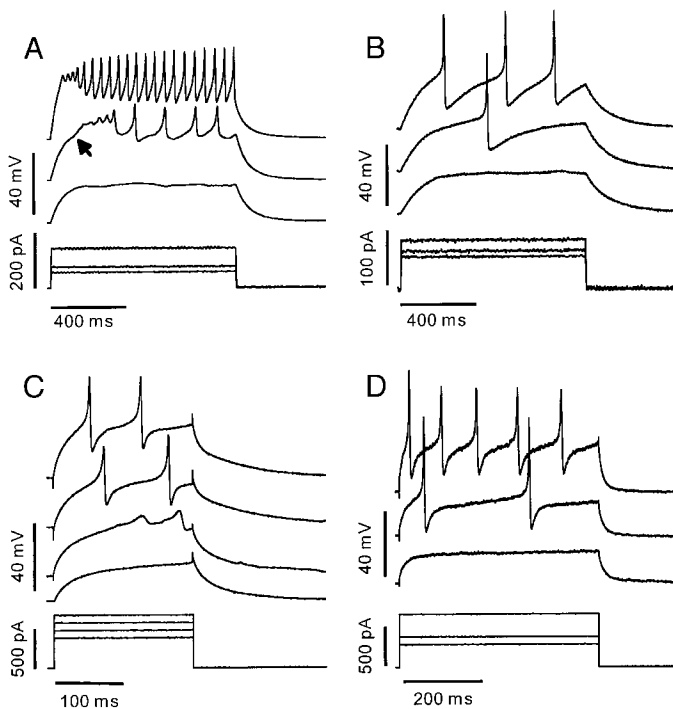


FIG. 3. Excitable properties of the muscle cells in dissociated muscle fibers (A and B) and the innervated muscle preparation (C and D). Positive current injections induce 2 main types of regenerative activity. A and C show “oscillatory” cells, the oscillatory potentials of which develop into trains of low-amplitude spikes. ←, onset of slow regenerative potential. B and D show “spiky” cells that respond with a train of overshooting spikes.

3D) were observed in the innervated muscle preparation. This suggests that the excitable membrane properties of the cells are not drastically altered by the dissociation or recording procedures.

An important functional issue is whether or not the longitudinal and transverse muscle fibers differ in their electrical properties. We found no significant differences in either the excitable or passive properties in the innervated muscle preparation (Table 1).

Muscle cells are electrotonically compact

Double whole cell recordings were performed on three dissociated muscle fibers to assess the spatial integrative properties of the muscle fibers (see *inset* in Fig. 4). The voltage responses recorded by the two micropipettes were identical over the whole range of voltage waveforms as well as during active spike generation (Fig. 4). Thus the muscle fibers appear to be isopotential cells and can serve as linear spatial integrators of synaptic inputs. On the basis of the input resistance, time constant and the dimensions of the cell ($900 \times 12 \mu\text{m}$),

we calculated a specific membrane resistance of $93 \text{ K}\Omega \cdot \text{cm}^2$ and a specific capacity of $1.55 \mu\text{F}/\text{cm}^2$. Assuming cytoplasmic resistivity of $70 \Omega \cdot \text{cm}$ (Laurienti and Blankenship 1996), the space constant of such fiber is 7.9 mm.

Muscle cells are innervated by three distinct types of excitatory synaptic inputs

Spontaneous postsynaptic potentials (sPSPs) are shown in Fig. 5A. Some of these are exceptionally large, as also found in squid fin and mantle muscle cells (Stockbridge and Stockbridge 1988). In contrast to these squid muscles, almost every recording from octopus arm muscle cells showed distinct classes of sPSPs that could be distinguished by their rise times and amplitudes (Fig. 5A). The two-dimensional distributions of the amplitudes and rise times (time from onset to peak) of the sPSPs are shown in Fig. 5C1. One group is formed by sPSPs with fast rise times (2–4 ms) and large amplitudes ($\leq 20 \text{ mV}$, Fig. 5C1, *). This group is clearly distinct from a large class of sPSPs with broadly skewed rise times (4–16 ms) and relatively low amplitudes ($< 10 \text{ mV}$). The distributions of rise times and amplitudes of the slow sPSPs are not uniform and can be viewed as combinations of two groups (Fig. 5C1, ** and ***).

Postsynaptic potentials were evoked by stimulating the lateral nerve roots (see METHODS and Fig. 1). Suprathreshold stimulation, at $\sim 50\%$ above PSP threshold intensity, ensured repeated activation of the same population of motor neurons. Nerve stimulation also revealed three classes of synaptic inputs. These were especially clear under conditions of low probability of release, which allow monitoring of single release events. These conditions were created by lowering the Ca^{2+} concentration in the bathing solution to 2 mM (Fig. 5B).

The traces in Fig. 5B show PSPs evoked by double pulse stimulation. These nerve-evoked PSPs are very similar to the sPSPs recorded in the same cell (Fig. 5A). The amplitude and rise-time distributions of the evoked (Fig. 5C, 2 and 3) and spontaneous PSPs (Fig. 5C1) clearly show three clusters with the three peaks similarly located on the rise time axis. The upward amplitude expansion of the three clusters of the evoked PSPs (Fig. 5C, 2 and 3), in comparison with the spontaneous PSPs (Fig. 5C1), can be explained by the summation of multiple releases, which would be predicted to be $\sim 20\%$ at this probability of release (45% failures). A further difference is that the population of small amplitude spontaneous PSPs is evoked very rarely by stimulation.

There was no significant difference in the amplitude versus rise-time distributions of the sPSPs in the transverse and longitudinal muscle fibers (cf. Fig. 6, A and B), suggesting that both muscle groups are similarly innervated. The sPSPs' frequency, which was variable among different muscle cells, could be elevated by increasing the tonicity of the ASW with

TABLE 1. Longitudinal and transverse muscle cells in innervated muscle preparations have similar active and passive membrane properties

	Resting Potential, mV	Input Resistance, M Ω	Membrane Time Constant, ms	Oscillatory/Spiky Cells
Longitudinal cells	-68.9 ± 4.3 (31)	31.9 ± 12 (9)	30.3 ± 18.5 (5)	5/8
Transverse cells	-67.3 ± 7.2 (30)	32.5 ± 15 (6)	25.3 ± 21.4 (10)	3/5
Two-tail <i>t</i> -test (<i>P</i>)*	0.374	0.939	0.655	

The number of measurements appears in parentheses. * *P* gives the level of significance.

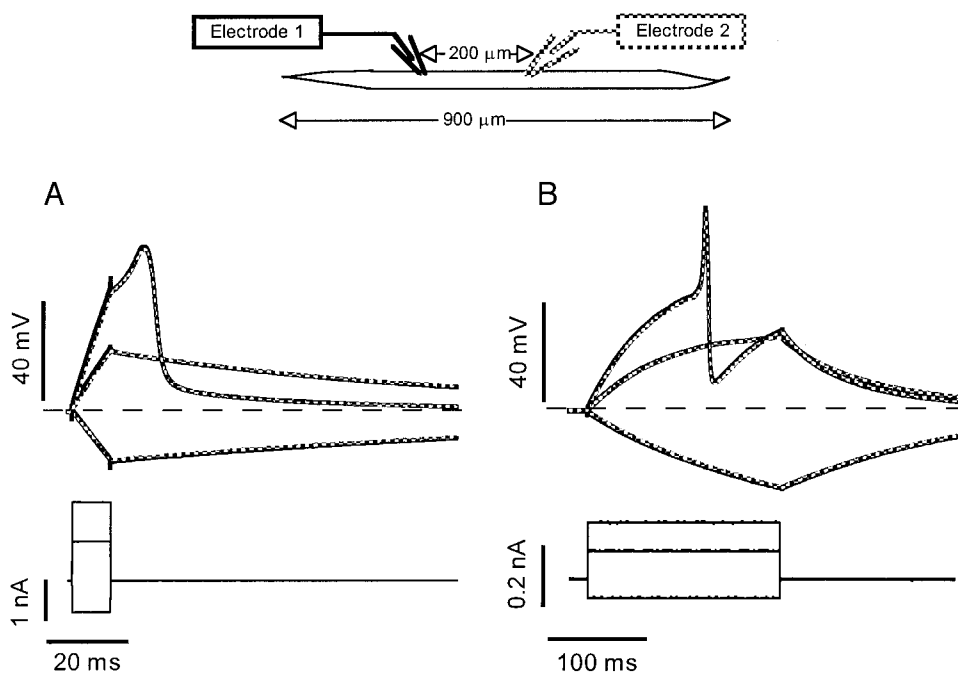


FIG. 4. Muscle fibers are very compact electrically. Two electrodes, in whole cell configuration, were attached to a cell 0.9 mm long at the positions indicated in the schematic *inset*. *A*: current steps of 10-ms duration injected through electrode 1 (continuous line), produced identical responses in electrode 2 (stippled line). Small 2 mV difference in membrane potential was adjusted to the average of -69 mV. Note that it was only possible to distinguish between the 2 traces because of the imperfect bridge balance and fast onset artifacts of electrode 1. *B*: as in *A* but with current pulses of 200-ms duration. There is no appreciable attenuation of passive responses, nor conduction delay of active responses along the 0.2-mm separation between the electrodes.

sucrose. This treatment has been found to increase the frequency of miniature PSPs by a mechanism independent of external Ca^{2+} concentration (Fatt and Katz 1952; Manabe et al. 1992; Mochida et al. 1998; Shimoni et al. 1977). Figure 6, *A1* and *B*, *I* and *2*, are derived from experiments with ASW to which 0.5 M sucrose was added. The sPSP distributions obtained under these conditions were not qualitatively different from those obtained under normal conditions (cf. Fig. 6*A*, *2* and *3*, and *B3*). Sucrose therefore was added to increase the sPSP sample in various experiments.

Several findings suggest that the sPSPs are equivalent to "miniature postsynaptic potentials (mPSPs)" and therefore represent the random release of synaptic vesicles ("quanta"). First, the probability of occurrence of the spontaneous sPSPs appears to be random. Second, sPSP frequency and amplitude did not change significantly after superfusion with TTX, which abruptly inhibited evoked release. It is less likely that sPSPs are due to spontaneous Ca^{2+} spikes as lowering Ca^{2+} concentration affected neither the amplitude nor the frequency of sPSPs. Third, under conditions of low release probability, the size of the single unit of the different classes of evoked PSPs matched the amplitude and shape of the spontaneous PSPs (Fig. 5) and, in some cases (e.g., Fig. 9), it is possible to discern discrete large units that comprise nerve-evoked release. And finally, as described in the preceding text, increasing the osmolarity of the ASW by adding sucrose elevated the frequency without affecting the amplitude distribution of the sPSPs. However, we cannot exclude the possibility that the sPSPs, especially the large and fast sPSPs, are composed of multiple vesicular releases. Indeed, the presence of a group of fast but low amplitude sPSPs (e.g., Figs. 5*C1* and 6*B1*) may represent a class of such subvesicles or, alternatively, input from another unidentified source. Subminiatures and giant miniature PSP have been described in several studies (see for review, Van der Kloot 1991). Our electron microscopic studies, however, show conventional small (30–50 nm) clear core vesicles at areas of

dense pre- and postsynaptic membrane junctions (unpublished observations).

Properties of the different classes of synaptic inputs

We next examined the pharmacology, ionic mechanisms, and plastic properties of the different neuromuscular connections to evaluate possible differences in the functions of the various synaptic inputs.

DECAY TIME COURSE OF THE PSPs. To further characterize the different synaptic inputs and to assess the electrical dimensions of the muscle cells in innervated muscle, the decay of the synaptic and passive potentials were analyzed. A slow PSP, fast PSP and the response to current injection are shown in Fig. 7*A* after normalization and alignment of the peaks. The decay of the passive potential and fast PSP demonstrated a good overlap, whereas the slow PSP decayed more slowly. The semilogarithmic plot in Fig. 7*B* shows that the main part of the decay phase of the passive and fast PSP, i.e., after ~ 10 ms, can be fitted with a single exponent, indicating a finite and relatively short electrotonic length of the cell (Rall 1969).

In contrast, the slow PSP does not show an initial fast decay, and the exponential part of the decay is much slower than the membrane time constant (Fig. 7*B*). In the example in Fig. 7*C*, the distribution of the half-decay, time of the sPSPs shows a cluster of fast rise-time sPSPs the half-decay time of which is very close to that of the passive decay (\rightarrow). The sPSPs with rise times longer than ~ 5 ms have a slower and broad distribution of half-decay times with some positive correlation ($r = 0.421$) between the rise time and half-decay time. Figure 7*D* summarizes six such analyses and reveals a correlation of close to one between the half-decays of the fast sPSPs and passive potentials. In addition, it shows the small SD of the fast decay in comparison to the large SD of the slow sPSPs. The similarity in half-decay time of the fast PSPs and passive potentials indicates a short electrical distance between the synapse and the electrode. Because it is hard to believe that the electrodes

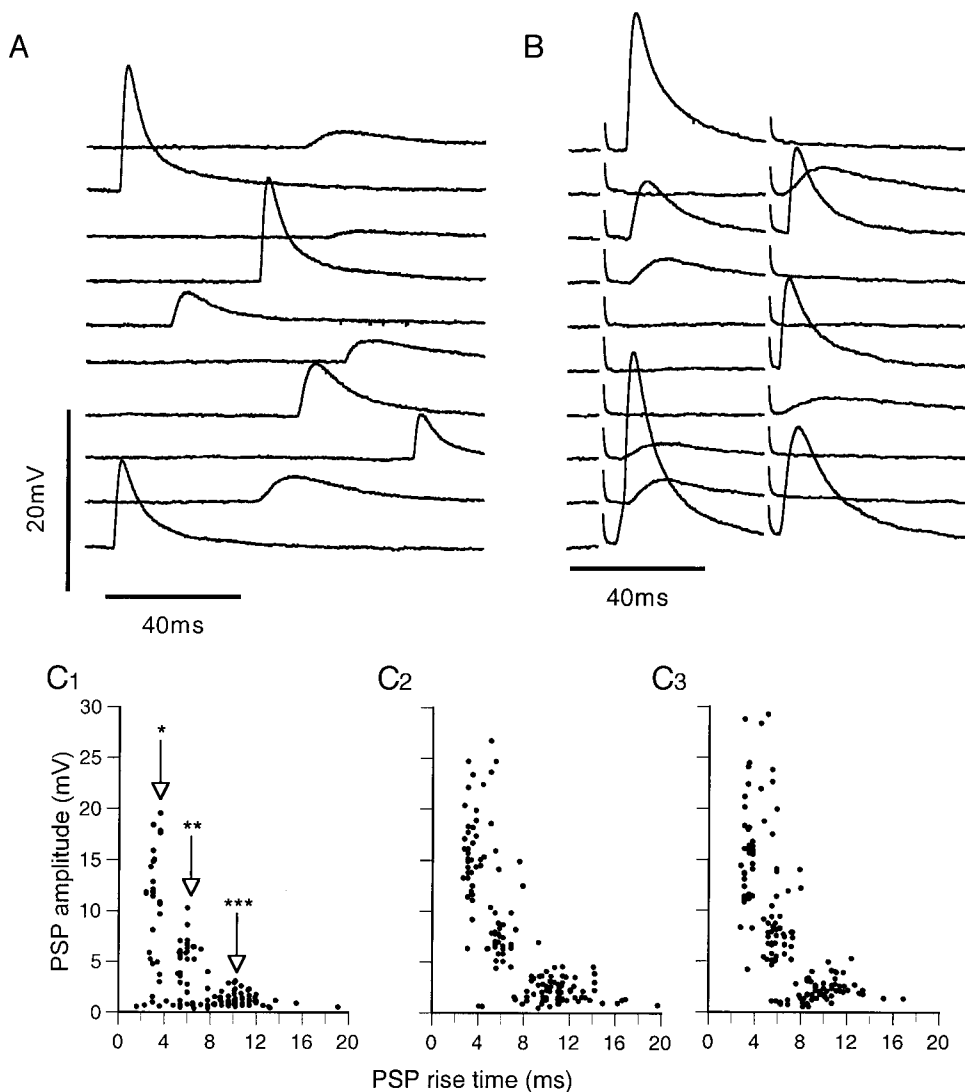


FIG. 5. Spontaneous and nerve-evoked activity recorded in the innervated muscle preparation reveals 3 classes of synaptic potentials. *A*: traces displaying the various types of spontaneous postsynaptic potentials (sPSPs) recorded in a transverse muscle cell. *B*: postsynaptic potentials (PSPs) in the same cell evoked by twin pulse stimulation in low Ca^{2+} concentration (2 mM), which reduces probability of release and allows detection of single events. *C*: analysis of the distribution of the amplitude vs. rise time (from onset to peak) of the spontaneous PSPs (*C1*) and the PSPs evoked by the 1st (*C2*) and 2nd (*C3*) stimulus. Three clusters (*C1*, *, **, and ***) can be seen at the same rise-time windows.

were at the same physical distance from the synapses in all recordings, a more plausible explanation is a short electrical length, as would be expected in electrically compact cells. Both the longer decay time constant (Fig. 7, *A* and *B*) and the much longer and variable half-decay time (Fig. 7, *C* and *D*) of the slow PSPs imply that the slower decay of this potential involves a current source and is not a passive phenomenon. Such a current can result from a long and variable duration of the synaptic current due, for example, to long channel openings (or bursts) or to slow transmitter removal/degradation processes, all of which can follow an exponential time course.

REVERSAL POTENTIALS. The reversal potential of the different synaptic inputs reveals whether they function as excitatory or inhibitory inputs. Figure 8*A* shows the amplitude-rise-time distribution of sucrose-induced sPSPs at five different membrane potentials imposed by DC current injection. To estimate the reversal potential of each class of sPSP, the potentials first were separated into three rise-time groups, fast, moderate, or slow. The rise-time windows marked in Fig. 8*A*, left, were chosen to minimize overlap between the three groups. The dependence of average sPSP amplitude on membrane potential was evaluated by linear regression for each rise-time window (Fig. 8*B*), and the reversal potential

was estimated by extrapolating to zero amplitude. The error was evaluated by resampling the data using the bootstrap method (Manly 1997) to estimate the SD of the intercept. The reversal potential (\pm SD) of the fast synapse was -4.2 ± 20.8 mV, the moderate PSP reversed at -0.1 ± 13.8 mV, and the slow PSP at $+8.7 \pm 24.1$ mV.

To compare the reversal potentials of the different synaptic inputs, we pooled and averaged the reversal potentials estimated from the evoked and spontaneous PSPs. This was possible because fairly good evidence suggests that they have similar postsynaptic properties and, most likely, are originating from the same synapses (see Figs. 5–7 and the pharmacological characterization in the following text). The average reversal potential of the fast PSP, at -11.3 ± 3.4 mV (mean \pm SE; $n = 10$), was not significantly different ($P = 0.729$, *t*-test) from -13.2 ± 3.7 mV ($n = 6$) for the moderate PSP. In the few cases where the reversal potential of the slow PSP could be measured, it was positive to the resting potential ($-35, 10, 30$ mV, mean = 1.7 ± 19 mV; $n = 3$). We never encountered cases where synaptic potentials actually reversed as a result of depolarization. Moreover all the extrapolated reversal potentials were positive to the thresholds for spike initiation. Thus it

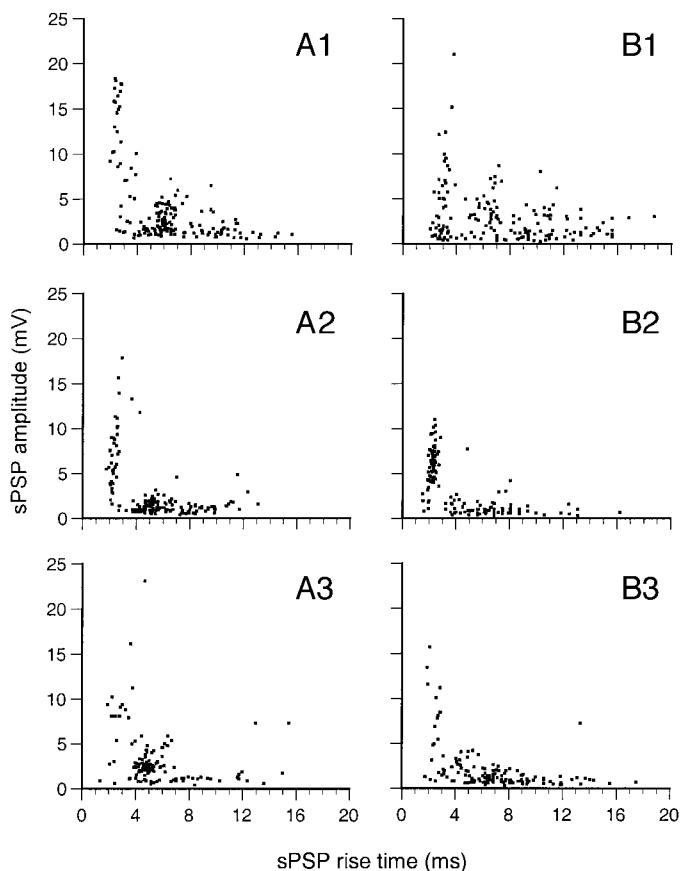


FIG. 6. Distribution of spontaneous PSPs amplitudes vs. rise times reveals similar patterns in different muscle cells and preparations. *A*, 1–3: sPSP distributions in 3 transverse muscle cells. *B*, 1–3: similar to *A* for 3 longitudinal muscle cells. Note the similar distributions in the longitudinal and transverse muscle cells, both when sPSPs were recorded in normal artificial seawater (ASW; *A*, 2 and 3, and *C*3), or in ASW with sucrose (*A*1 and *B*, 1 and 2).

seems reasonable to conclude that all the synaptic potentials were excitatory postsynaptic potentials.

An additional, independent method was used to estimate the reversal potential of the fast PSP. The large amplitude of the unitary events (≤ 25 mV in some cells) suggests a nonlinear summation when several units are simultaneously liberated. In the experiment shown in Fig. 9, it was relatively easy to evoke only the fast PSP by adjusting the stimulus level. The PSP amplitude varied greatly, from failures to initiation of spikes (Fig. 9A). This indicates the low probability of release, even at normal Ca^{2+} concentration. Three peaks (\rightarrow) can be distinguished in the PSP amplitude histogram in Fig. 9B; these most likely correspond to PSPs composed of one, two, or three quanta. The dependence of the amplitude of a single quantum on membrane potential can be estimated by plotting the voltage differences between successive peaks as a function of the membrane potential of the lower peak. This dependence showed a linear relationship, which extrapolated to a reversal potential of -19.5 mV (Fig. 9C). This result falls at the lower range of average reversal potential estimated by current injections (see preceding text). Possible reasons may be a saturation of postsynaptic receptors (Frerking and Wilson 1996) and/or membrane rectification at higher membrane potentials. [Note that the 1st and 2nd peaks extrapolate to a more positive potential (-12 mV).]

TWIN PULSE MODULATION OF TRANSMITTER RELEASE. Twin pulse facilitation can be used to characterize the activity-dependent modulation of transmitter release and also allows analysis of mechanisms of transmitter release (for reviews, see Parnas and Parnas 1994; Zucker 1989). Because we could not reliably stimulate each motor neuron separately, we studied twin pulse modulation of release using suprathreshold stimulation.

The average postsynaptic responses induced by twin pulse with varying interstimulus intervals are shown in Fig. 10B, with the ratio of the amplitudes of the second to the first PSPs giving the level of modulation. The results of three such experiments, performed in normal Ca^{2+} concentration, are summarized in Fig. 10C. Only marginal levels of modulation were detected, and there was no consistent dependence on the interstimulus interval. For example, in Fig. 10C (\bullet), there is practically no facilitation (1.05 at 50-, 1.02 at 80-, and 1.06 at 100-ms intervals). There appeared to be a small depression in one experiment in which shorter intervals were tested (Fig. 10, A–C, \circ). This depression also may be due to a reduction in driving force. In another example (Fig. 10C, \blacksquare), facilitation was followed by depression.

The level of twin pulse modulation of each of the three classes of synapses was investigated using the amplitude-rise-time distributions of the first and second PSP. Figure 10A shows the large variability in amplitude and rise time of the individual responses that results both from the large differences in amplitude and shape of the fast and slow PSPs and from the relatively low probability of release. In the experiment shown in Fig. 10, A–C, a facilitation of 1.16 is evident at the 80-ms interval (Fig. 10C, \circ). Comparing the distributions of the first and second PSPs at this interval reveals that the pattern of PSPs distribution did change with a shift toward faster and larger PSPs in the second PSP (Fig. 10D). This result suggests that the compound average facilitation at this interval is mainly due to the facilitation of the larger fast PSP. Indeed, considering a possible nonlinear summation, the 20% increase in the number of fast events in the second PSP can account for the 16% average facilitation seen at 80 ms interval (Fig. 10, B and C, \circ).

The tendency of the slow PSPs to demonstrate less facilitation than the fast PSPs is even more robust at low Ca^{2+} concentration, a condition which reduces probability of release but also enhances twin pulse facilitation (Parnas et al. 1982). In the example in Fig. 10E, there was about a 25-fold decrease in the average amplitude of the PSP elicited by the first stimulus after lowering Ca^{2+} concentration to 1 mM. The compound PSP now showed large facilitation, although it had not done so in normal ASW (Fig. 10C, \bullet). The second PSP at the 10-ms interstimulus interval was more than double the size of the first PSP. Facilitation declined by 50 ms and almost disappeared by 80 ms. As can be seen from the average records (Fig. 10E) and confirmed by counting single events (not shown), this facilitation is mainly due to the fast PSPs. An experiment in which only slow PSPs were evoked (Fig. 10F) directly demonstrates the lack of twin pulse modulation of release even at low Ca^{2+} concentration (see also Fig. 5).

These results suggest that the synaptic junctions in the octopus arm may be all classified as “fast synapses,” as they do not show robust facilitation at intervals that were effective in other neuromuscular systems (Hochner et al. 1991; Parnas and Atwood 1966; Zucker 1989).

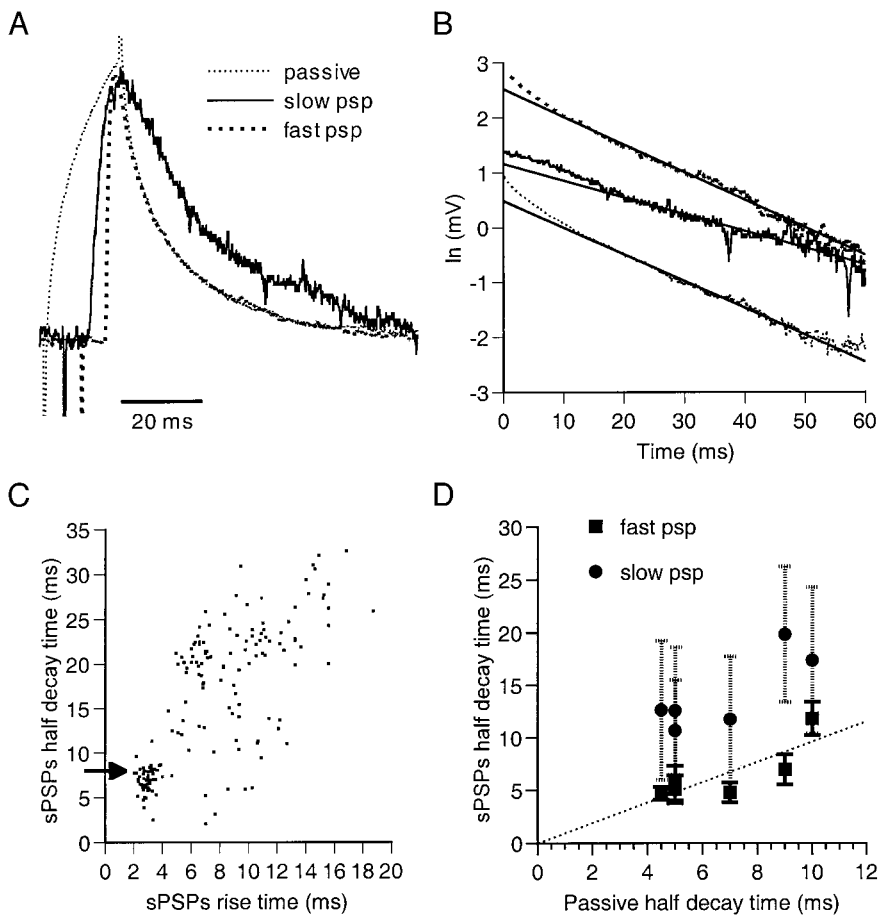


FIG. 7. Measurements of membrane time constants as a means for estimating the electrical dimensions of muscle cells in the innervated muscle preparation. *A*: slow and fast PSPs are displayed together with a low-amplitude passive response to current injection. PSPs are single events, the passive response is an average. Three responses are normalized and aligned at the peaks. Fast sPSP and the passive potential have a similar decay time course, whereas the slow PSP decay is significantly slower. *B*: semilogarithmic plot of the decay phases shows a similar behavior for the fast and passive potentials. After ~ 10 ms, the decay can be fitted with a single exponent corresponding to the membrane time constant. Slow PSP also can be fitted by a single time constant but longer than that of the passive potential and fast PSP. *C*: example for the distribution of sPSP half-decay time (the time from peak to 50% amplitude) as a function of sPSP rise time. Fast sPSPs have a decay time similar to the average half-decay of the passive potential (\rightarrow), whereas the slow sPSPs have broadly distributed half-decay times. *D*: summary of 6 experiments showing the correlation between the half-decay time of the passive potential and those of the fast and slow sPSPs. Error bars indicate SD. Linear regression line has a slope of 0.966, indicating similar half-decay of the passive and fast sPSP. Slow sPSPs have much longer and broader distribution of half-decay times.

PHARMACOLOGICAL ANALYSIS. Acetylcholine (ACh) has been identified as the neuromuscular transmitter in most studies in mollusks (Bone et al. 1982, 1995; Cohen et al. 1978; Kozak et al. 1996; McPherson and Blankenship 1991), although some reports suggest glutamate as a potential neuromuscular transmitter (Bone et al. 1982; Florey et al. 1985; Fox and Lloyd 1999). ACh receptor antagonists, hexamethonium, D-tubocurarine (dTC), and atropine were tested here to identify the neuromuscular transmitter in the octopus arm. The pharmacological experiments on the innervated muscle preparation required a relatively high range of drug concentrations (0.2–10 mM), possibly due to the fast local superfusion method of application (see METHODS); in addition, the muscle cells are packed densely (Bone et al. 1995; unpublished observations), and this may impede penetration of the drugs into deep muscle layers where the recorded cells most likely lie.

Local superfusion with hexamethonium (10 mM) blocked all types of PSPs with a slow recovery after washing (not shown, see Table 2). Perfusion with 2 mM hexamethonium led to a partial inhibition of spontaneous (Fig. 11) and evoked PSPs (not shown). Hexamethonium blockade appears to be accompanied by an apparent reduction in occurrence of sPSPs (Fig. 11, *B* and *C*), which may indicate presynaptic effects of the drug, but it also may be due to the difficulty in detecting the PSPs as they disappear into the noise. The logarithmic display in Fig. 11*B* shows an apparent parallel decline in the amplitudes of the fast sPSPs and the upper amplitude boundary of the slow sPSPs, possibly indicating similar relative potency of hexamethonium on the different PSPs. A consistent and spe-

cific effect of hexamethonium on spontaneous and evoked *fast* PSPs was the shortening of the rise time which accompanied the inhibition effect (Fig. 11*C*). This suggests activity-dependent blockage of the postsynaptic channels and/or change in channel kinetics.

The analysis of the effects of the three drugs is summarized in Table 2. All are reversible antagonists of both the evoked and spontaneous PSPs. The muscarinic antagonist, atropine, seems to be the most potent inhibitor of the three classes of PSPs. We could not detect a differential response to hexamethonium, dTC, or atropine on the two classes of slow PSPs, but these may be too subtle to allow detection. As shown in Table 2, hexamethonium causes shortening of the rise time of only the fast PSP, whereas dTC did not affect the rise times and atropine shortens all classes of PSPs. These differential effects on the time courses of the PSPs suggest a pharmacological difference between the fast and slow PSP classes.

Cross-inactivation experiments, in which the muscle was slowly exposed to 1 mM ACh, led to the suppression of all types of sPSPs. Similar experiments with glutamate did not affect the postsynaptic potentials. ACh added to the bath blocked the local muscle contractions evoked by nerve stimulation, while glutamate did not affect the contractions. These results further support ACh as the neuromuscular transmitter.

DISCUSSION

The results presented here provide the first analysis of the neuromuscular system of the octopus arm. They suggest that

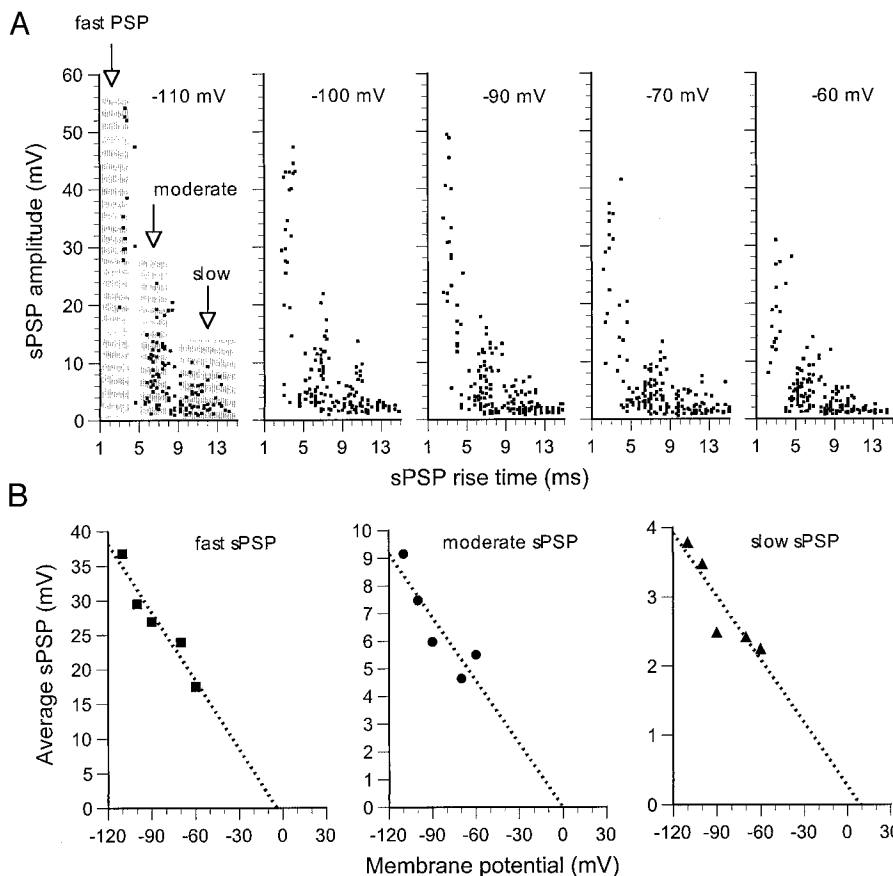


FIG. 8. Estimation of the reversal potentials of the 3 classes of PSPs. *A*: analysis of the amplitude vs. rise-time distribution of the sucrose-induced sPSPs at 5 membrane potentials (indicated in each inset) imposed by DC current injections. Resting membrane potential was -70 mV. Average amplitude of each class of sPSPs (fast, moderate, and slow sPSPs) was calculated by averaging all the PSPs included in the rise-time windows, indicated by the gray background in the left hand panel. *B*: estimation of the reversal potential by plotting the average amplitude of the sPSPs as a function of membrane potential. Extrapolated reversal potentials, obtained from linear regression, were -4.2 mV ($-r = 0.960$, $P = 0.0093$), -0.1 mV ($-r = 0.885$, $P = 0.046$), and $+8.7$ mV ($-r = 0.905$, $P = 0.034$) for the fast, moderate, and slow sPSPs, respectively.

some of the unique properties of this neuromuscular system reflect evolutionary adaptation for the efficient control of a muscular hydrostat. These include the small morphological and electrical dimensions of the muscle cells, the innervation of

each muscle cell by three classes of excitatory motor neurons, the lack of profound activity-dependent synaptic plasticity and the similarity in the properties of antagonistic longitudinal and transverse muscle cells.

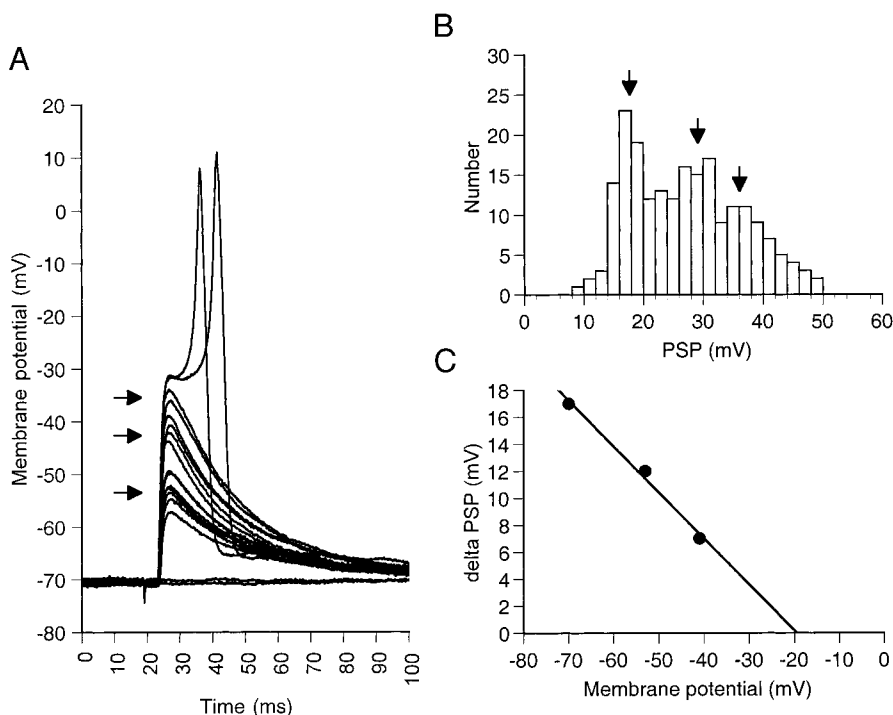


FIG. 9. Estimation of the fast PSP reversal potential from nonlinear amplitude summation. *A*: superposition of PSPs evoked by stimulating the motor nerve at a strength that activated only the fast PSP. In normal ASW, there was a large variation in PSP amplitude, from failure to a PSP that initiated a spike. *B*: PSP amplitude histogram reveals 3 peaks (\downarrow) corresponding to the levels indicated in *A*. This may be explained by multiple release of 1, 2, or 3 quanta. *C*: voltage increments induced by the 1st, 2nd, and 3rd quanta diminish as a function of the membrane potential in a linear relationship ($-r = 0.995$, $P = 0.063$, slope = -0.3414 ± 0.034 , intercept = -6.665 ± 1.901 mV), which extrapolates to the reversal potentials (-19.5 mV).

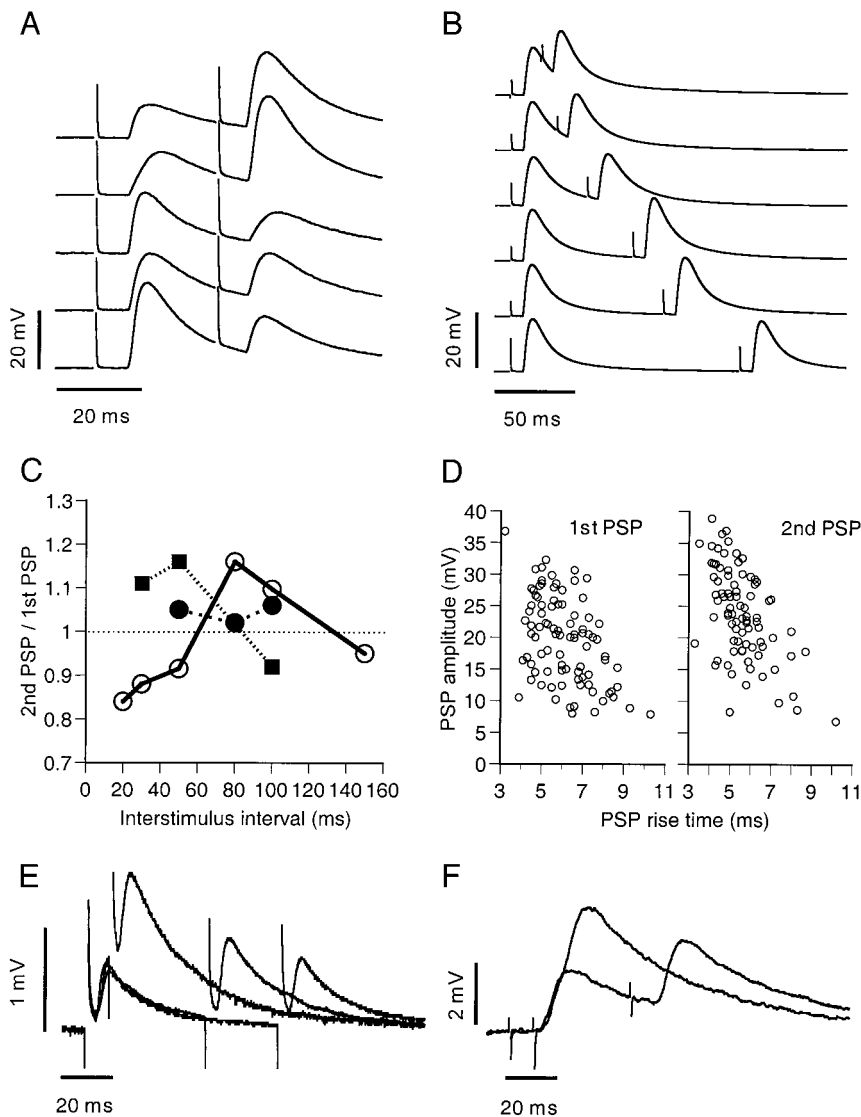


FIG. 10. Synaptic plasticity assessed by twin pulse modulation of release. *A*: selected individual traces demonstrating variability in PSP amplitude and rise time obtained in normal ASW. Motor nerve was stimulated with twin pulses at an interstimulus interval of 30 ms. *B*: average responses obtained at 6 different interstimulus intervals. Level of modulation is marginal, as summarized in *C* (\circ). *C*: summary of 3 such experiments demonstrating inconsistency and low level of modulation under normal Ca^{2+} conditions, as is typical for "fast" synapses. *D*: amplitude vs. rise-time distributions of the PSPs evoked by the 1st stimuli (1st PSP), and those by the 2nd stimuli (2nd PSP) in the same experiment as in *A*–*C* (\circ), at an interstimulus interval of 80 ms. There is a shift toward faster responses. *E*: large facilitation of fast PSP at short interstimuli interval is revealed in low Ca^{2+} concentration (1 mM). Records are averages that include many failures. *F*: experiment where only slow PSPs were evoked. As shown in the averaged records, no significant twin pulse facilitation was obtained, even in low Ca^{2+} (2 mM), and with a very short interval (10 ms).

Passive properties of the muscle cells

A most significant finding is the compact electrical dimensions of the muscle cells of both longitudinal and transverse muscle groups. The cells are virtually isopotential with very high-input resistance (Fig. 4). Indirect evidence suggests that this may be a general characteristic of cephalopod muscles (Bone et al. 1995; Gilly et al. 1996; Rogers et al. 1997; Stockbridge and Stockbridge 1988); as well, compact electrical dimensions are shown by the dissociated muscle fibers of the parapodial swim muscle (Laurienti and Blankenship 1996) and the buccal mass (Brezina et al. 1994) of the mollusk *Aplysia*,

although the latter cells are electrically coupled in the intact muscle (Cohen et al. 1978). The electrical compactness has functional implications for the control of the muscle activation as the entire muscle fiber is activated simultaneously. Unlike vertebrate striated muscle (e.g., Fatt and Katz 1951), the isopotentiality of the octopus muscle cell indicates that the regenerative membrane properties are not likely to serve the transmission of electrical signals along the muscle fibers.

We attribute the significant differences between the input resistances and time constants of the dissociated muscle cells, and those of innervated muscle fibers, to damage caused by the

TABLE 2. Summary of the effects of ACh receptor antagonists on the slow and fast PSPs

	Maximum Inhibition,* mM	Minimal Concentration,** mM	Relative Higher Potency (slow/fast)	Shortening of PSP Rise-Time (slow/fast)
Hexamethonium	10	2	same	fast
dTC	10	1	fast	none
Atropine	1	0.2	same	slow fast

Table provides a qualitative summary of 14 experiments (see METHODS and text). dTC, D-tubocurarine. * The concentration that leads to complete blockage or more than ~90% inhibition in experiments that had not reached steady state. ** The lowest tested concentration that produced a significant effect.

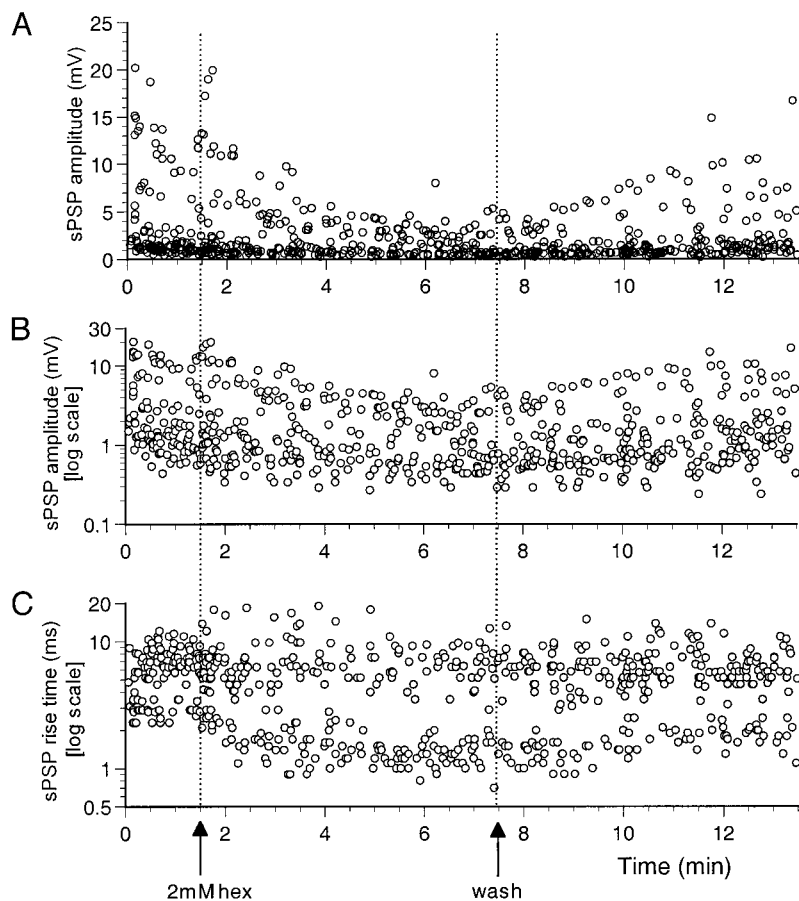


FIG. 11. Hexamethonium inhibits spontaneous sPSPs. *A*: sPSP frequency was elevated by superfusion with 0.5 M sucrose. Superfusion of 2 mM hexamethonium (hex) led to gradual reduction in sPSP amplitudes that recovered after washing (wash). *B*: same plot as in *A*, using a logarithmic scale for the sPSP amplitude to show slow and fast PSPs on the same plot and to assess the *relative* inhibitory effects of the drug on the different PSP classes. *C*: effect of hexamethonium on sPSP rise time (log scale). Inhibition was accompanied by shortening of the fast sPSPs rise time, whereas the rise time of the slow sPSPs was unaffected.

intracellular recording electrodes (Marty and Neher 1995). Although we have not found any morphological indications for gap junctions (unpublished observation), electrical coupling between muscle cells, as found in other mollusk muscles (Cohen et al. 1978), could be an alternative explanation. According to this explanation, the PSPs with low amplitude and slow time course may originate from fast PSPs in neighboring cells. Theoretically the degree of the DC coupling coefficient between coupled RC compartments can be estimated from the ratio of the areas under the PSPs (Rinzel and Rall 1974). The ratios of the areas under slow and fast PSPs suggest coupling coefficients between 1:3 for the moderate PSPs and 1:5 for the slow PSPs. This may indicate a relatively strong coupling between the muscle cells that could account for the large difference in input resistance.

On the other hand, several findings are incompatible with the mediation of the two slow groups of PSPs by electrical synapses. 1) The exponential decay of the slow PSPs is significantly slower than the membrane time constant calculated from the exponential decay of the passive potentials or from the fast PSPs (Fig. 7). This suggests that an active current participates in the decay phase of the slow PSPs (Rall 1964). Contrasting with the slow PSPs, the striking similarity in the decay phases of the passive and fast PSPs strongly suggests a passive decay for the fast PSP, and it therefore cannot serve as a current source for the active decay of the slow PSPs. This suggests differences in synaptic mechanisms that cannot be attributed to electrical coupling. 2) The pharmacological results, especially the fact that each drug caused a specific and different combi-

nation of effects on PSP rise times, indicate the presence of synaptic inputs with pharmacologically distinct postsynaptic ACh receptors for the slow and fast PSPs (Fig. 11, Table 2). 3) The estimated reversal potentials of the different classes of PSPs lie in the same range; with electrical coupling, the reversal potential of the synapse originating in the neighboring cells would be higher due to voltage and current attenuation. For example, the DC coupling, estimated in the preceding text, suggests a three to five times more positive reversal potential for a PSP originating in the coupled cell (+110 mV for moderate PSPs to +300 mV for the slow PSPs), which clearly exceeds the range of variability of our results. And 4) the fact that the slow and fast PSPs show different twin pulse facilitation properties at low Ca^{2+} concentration (Fig. 10, *E* and *F*) also supports their uniqueness. We therefore suggest that the muscle cells in the octopus arm are unlikely to function as a syncytium of highly coupled muscle cells. However, because our analysis centers on the properties of the different PSPs, we cannot exclude the possibility of a low coupling, too weak for transmission of a significant synaptic potential, that could serve to coordinate activity in an ensemble of muscle cells.

Active membrane properties of the muscle cells

The presence of active membrane properties in octopus arm muscle fibers suggests that the mechanical output of the muscle is not a simple function of the synaptic activity at all voltage ranges. We found that octopus muscle cells are capable of generating a repertoire of active membrane potentials, which

include overshooting action potentials, oscillations, and slow regenerative potentials (Fig. 3). Because the electrical compactness of the muscle fibers implies that the electroresponsiveness of the cells is not required for spreading excitability along the cell, these properties are more likely involved in the activation of the contractile machinery.

The threshold for activation of the regenerative potentials is relatively high (approximately -40 mV with resting potential close to -70 mV). Muscle contractions can be generated at membrane potentials below this threshold (unpublished observation), ensuring a wide potential range where synaptic inputs can directly control muscle contraction. The regenerative processes, therefore may come into play when vigorous contractions are required. The nature of the active currents are still unknown; in cephalopods, fast sodium currents (Gilly et al. 1996) and an L-type Ca^{2+} current have been shown to mediate muscle contraction (Rogers et al. 1997). If slow Ca^{2+} currents mediate some of the regenerative responses observed here, for example, the slow regenerative potentials, then these currents, together with oscillations or trains of spikes, may serve as a very powerful mechanism for introducing Ca^{2+} . This may be an effective solution for muscle cells that lack a specialized system for transferring the signal into the cell, such as the T-system found in other muscular systems (Bone et al. 1995).

Neural control of muscle activation

On the basis of morphological studies, Young (1965) estimated that 3.8×10^5 motor neurons innervate the intrinsic muscles of each arm via the numerous nerve roots projecting from the axial nerve cord which runs along the arm (Graziadei 1971; Martoja and May 1956). Our physiological findings support a high level of localization in the neural control of these muscles; stimulation of the lateral nerves (Fig. 1) evokes PSPs only in muscle cells close to the stimulated nerves (unpublished observations). Further morphological investigation is needed to characterize number, types, size, and innervation pattern of the neurons in these nerve roots.

In contrast to the muscle cells of other invertebrates (Bullock and Horridge 1965; Hoyle 1977), the cells in the octopus arm are isopotential, and thus each synaptic input can control the membrane potential of the entire cell via a single localized synaptic junction. This proposition is supported by the similarity in membrane time constant calculated from the decay of fast PSP and passive voltage decay (Fig. 7). Indeed, our unpublished results show that the number of synaptic junctions is comparable with the number of nuclei in cross-sections of the arm muscles. This morphological finding suggests a low density of innervation of each muscle cell.

Each muscle fiber, in both longitudinal and transverse muscles, receives three types of synaptic inputs. In polyneuronal neuromuscular systems, the synaptic inputs to one muscle cell may be excitatory or inhibitory; they may be "fast" (phasic), i.e., large amplitude and nonfacilitating, or "slow" (tonic), i.e., low-amplitude and facilitating (Parnas and Atwood 1966). The situation in the octopus arm appears simpler. First, the estimated PSP reversal potentials indicate that the innervation is exclusively excitatory. Second, despite the difference in amplitude, all the synaptic inputs are phasic synapses showing only modest twin pulse modulation. Thus simple postsynaptic

summation serves as the main mechanism for transforming the presynaptic activity into muscle action.

The fast PSPs are composed of very large, probably quantal units, and thus few are required to activate the muscle; the slow PSPs are composed of smaller unitary responses, and temporal summation of such PSPs may be effective in activating the muscle. The low-amplitude PSPs have a slower time course; this increases their capacity for postsynaptic summation. Thus from a functional point of view, one may hypothesize that the fast PSPs participate in phasic and vigorous responses that require active currents generated at relatively high membrane potentials (-40 to -30 mV). On the other hand, trains of slow PSPs, with their slow time course and low amplitude, may mediate sustained muscle contraction by regulating the membrane potentials below the threshold for active currents (between -70 and -40 mV). Interestingly, our electromyogram (EMG) and modeling studies (Aharonov et al. 1997; Gutfreund et al. 1998) suggest an important role for tonic regulation of muscle stiffening in the generation of arm movements.

A unique feature of the fast motor neuron input to the octopus arm muscle is the unusually large unitary postsynaptic response. Stockbridge and Stockbridge (1988) obtained similar results in the neuromuscular system of the fin and mantle of the squid, and so this may be a general property of cephalopod neuromuscular systems. These large PSPs cannot be attributed solely to high-input resistance of the muscle fibers because we found a second class of slow PSPs with lower amplitude. The functional role of this large unitary response needs to be explored further; nevertheless, large quantal size, together with the low probability of release (Fig. 9), suggest a stochastic mechanism for recruitment of muscle fibers. This is possibly an adaptive mechanism for the control of a system composed of many small muscle cells. In a system composed of many small cells with the same function, the force generated can be determined by the number of cells activated, and not only by the level of activation.

Acetylcholine is the probable neuromuscular transmitter in the octopus arm muscles

Acetylcholine and L-glutamate have been suggested as excitatory neuromuscular transmitters in cephalopods (Bone et al. 1982, 1995; Florey 1985) and other mollusks (Cohen et al. 1978; Fox and Lloyd 1999; Kozak et al. 1996; McPherson and Blankenship 1991). Indirect experiments led Bone et al. (1982) to suggest ACh as the putative transmitter in the octopus arm. Our results directly support the involvement of ACh in the neuromuscular synapses in the octopus arm. The ACh antagonists, hexamethonium, curare, and atropine, block both spontaneous and nerve-evoked fast and slow PSPs. In addition, nerve-evoked contractions were inhibited by ACh, but L-glutamate had no effect. The postsynaptic receptors of the octopus arm muscles resemble those of the cationic ACh receptor channels in *Aplysia* ARC muscle (Cohen et al. 1978; Kozak et al. 1996; Laurienti and Blankenship 1999), which, unlike other invertebrate neuromuscular junctions, are blocked by hexamethonium (Colquhoun et al. 1991). As in other invertebrate neuromuscular ACh receptors (see Colquhoun et al. 1991), the muscarinic antagonist, atropine, and the nicotinic blocker, curare, were effective in blocking the neuromuscular junctions (but see following text).

In mollusks, ACh receptors have been found to mediate both excitatory (nonspecific cationic currents) and inhibitory (chloride) currents (Gardner and Kandel 1977; Kehoe and McIntosh 1998; Kozak et al. 1996; Laurienti and Blankenship 1999), but here only functionally excitatory connections were found. The reversal potential of these synaptic potentials (about -10 mV) may fit with two mechanisms described in ACh-mediated neuromuscular transmission. One involves chloride and cationic (Na^+) currents (ARC muscle of *Aplysia*) (Kozak et al. 1996), whereas the second involves a nonspecific cationic current (K^+ and Na^+), as in vertebrate neuromuscular junctions (Takeuchi and Takeuchi 1960), neuronal nicotinic receptors in mollusks (Ascher et al. 1978), and ACh-mediated depolarizing currents in the parapodial muscle of *Aplysia brasiliensis* (Laurienti and Blankenship 1999).

The specific drug actions on the time course of the different classes of PSPs suggest the existence of several types of postsynaptic ACh receptors. dTC did not affect the rise time of the fast and slow PSPs, whereas hexamethonium caused a shortening of the fast PSP only and atropine shortened all PSPs. No significant changes in passive membrane properties were observed, and thus the faster rise of the PSP is most likely due to shortening of the synaptic currents. This shortening effect is most probably due to blocking agents binding to the open channel. Such behavior is characteristic for the interaction of several ACh receptor antagonists with other molluscan neuronal cationic channels, especially dTC and hexamethonium (Kehoe and McIntosh 1998). In contrast to the pharmacological differences between the fast and slow PSPs, none of the antagonists used so far demonstrated any significant differences between the two classes of slow PSPs that were identified physiologically.

Implications of neuromuscular organization for the function of the octopus arm

The main feature of the octopus arm is that it does not contain a rigid skeleton, forcing the muscle tissue to serve both as a dynamic skeletal support and for movement generation. This is achieved by keeping the volume of the arm constant (Kier and Smith 1985). Mechanically this structure allows the arm unlimited degrees of freedom because the arm can elongate, shorten, twist, and bend at any point along it. Several of the results reported here may represent adaptive mechanisms for the control of flexible muscular hydrostats.

The octopus arm does not show several features that endow the neuromuscular systems of other invertebrates with nonlinear transformation properties (Bullock and Horridge 1965; Hoyle 1977). First, the synaptic control of membrane potential does not include postsynaptic inhibition. Second, the integrative properties of the muscle cells are linear due to the linear membrane properties and the isopotentiality of the cells. Third, the identified synaptic inputs do not possess profound activity-dependent plastic properties. Therefore it is tempting to speculate that this design leads to rather simple and more direct transformation of neural activity (spike frequencies) into muscle action.

The similarities between the functional units of the longitudinal and transverse muscle groups include the morphological structure of the muscle cells, their passive and active membrane properties, their pattern of innervation, and the properties

of their synaptic connections. Kier (1985) similarly has found that squid arms, which are involved mainly in bending, are built of muscle cells of similar ultrastructural characteristics. In contrast, in the elongating tentacles, the transverse muscle cells show morphological adaptation consistent with the major role of the transverse muscle group in tentacle elongation. The findings presented in this study extend this organizational principle to the neuronal and physiological levels.

We thank N. Feinstein for the morphological data, Dr. Graziano Fiorito, from the Stazione Zoologica di Napoli, for collaboration and contributions to various aspects of this research, Dr. Jenny Kien for critical readings of this manuscript, Prof. Yosef Yarom for valuable comments and discussions during the course of this research, and Prof. Idan Segev for advice on analyzing the electrotonic properties.

This work was supported by the Office of Naval Research (N00014-94-1-0480), by the Israel Academy of Sciences and Humanities (190/95-1), and by the United States-Israel Binational Science Foundation (95-00170).

Address reprint requests to B. Hochner.

Received 9 July 1999; accepted in final form 28 October 1999.

REFERENCES

- AHARONOV, R., ENGEL, Y., HOCHNER, B., AND FLASH, T. A dynamic model of the octopus arm (Abstract). *Neurosci. Lett. Suppl.* 48: S1, 1997.
- ASCHER, P., MARTY, A., AND NEILD, T. O. The mode of action of antagonists of the excitatory response to acetylcholine in *Aplysia* neurones. *J. Physiol. (Lond.)* 278: 207–235, 1978.
- BONE, Q., BROWN, E. R., AND USHER, M. The structure and physiology of cephalopod muscle fibres. In: *Cephalopod Neurobiology*, edited by N. J. Abbot, R. Williamson, and L. Maddock. New York: Oxford Science Press, 1995, p. 301–329.
- BONE, Q., PACKARD, A., AND PULSFORD, A. L. Cholinergic innervation of muscle fibres in squid. *J. Mar. Biol.* 62: 193–199, 1982.
- BREZINA, V., EVANS, C. G., AND WEISS, K. R. Characterization of the membrane currents of a model molluscan muscle, the accessory radula closer muscle of *Aplysia californica*. I. Hyperpolarization-activated currents. *J. Neurophysiol.* 71: 2093–2112, 1994.
- BULLOCK, T. H. AND HORRIDGE, G. A. *Structure and Function in the Nervous Systems of Invertebrates*. San Francisco, CA: W. H. Freeman and Co., 1965.
- COHEN, J. L., WEISS, K. R., AND KUPFERMANN, I. Motor control of buccal muscles in *Aplysia*. *J. Neurophysiol.* 41: 157–180, 1978.
- COLQUHOUN, L., HOLDEN-DYE, L., AND WALKER, R. J. The pharmacology of cholinergic receptors on the somatic muscle cells of the parasitic nematode *Ascaris suum*. *J. Exp. Biol.* 158: 509–530, 1991.
- FATT, P. AND KATZ, B. An analysis of the end-plate potential recorded with an intra-cellular electrode. *J. Physiol. (Lond.)* 115: 320–370, 1951.
- FATT, P. AND KATZ, B. Spontaneous subthreshold activity at motor nerve endings. *J. Physiol. (Lond.)* 117: 109–128, 1952.
- FLOREY, E., DUBAS, F., AND HANLON, R. T. Evidence for L-glutamate as a transmitter substance of motoneurons innervating squid chromatophore muscles. *Comp. Biochem. Physiol. C Comp. Pharmacol.* 82C: 259–268, 1985.
- FOX, L. E. AND LLOYD, P. E. Glutamate is a fast excitatory transmitter at some buccal neuromuscular synapses in *Aplysia*. *J. Neurophysiol.* 82: 1477–1488, 1999.
- FRERKING, M. AND WILSON, M. Saturation of postsynaptic receptors at central synapses? *Curr. Opin. Neurobiol.* 6: 395–403, 1996.
- GARDNER, D. AND KANDEL, E. R. Physiological and kinetic properties of cholinergic receptors activated by multiaction interneurons in buccal ganglia of *Aplysia*. *J. Neurophysiol.* 40: 333–348, 1977.
- GILLY, W. F., PREUSS, T., AND MCFARLANE, M. B. All-or-none contraction and sodium channels in a subset of circular muscle fibers of squid mantle. *Biol. Bull.* 191: 337–340, 1996.
- GOSLINE, J. M., STEEVES, J. D., HARMAN, A. D., AND DEMONT, M. E. Patterns of circular and radial mantle muscle activity in respiration and jetting of the squid *Loligo opalescens*. *J. Exp. Biol.* 104: 97–109, 1983.
- GRAZIADEI, P. The nervous system of the arms. In: *The Anatomy of the Nervous System of Octopus Vulgaris*, edited by J. Z. Young. Oxford, UK: Clarendon Press, 1971, p. 44–61.

- GUTFREUND, Y., FLASH, T., FIORITO, G., AND HOCHNER, B. Patterns of arm muscle activation involved in octopus reaching movements. *J. Neurosci.* 18: 5976–5987, 1998.
- GUTFREUND, Y., FLASH, T., YAROM, Y., FIORITO, G., SEGEV, I., AND HOCHNER B. Organization of octopus arm movements: a model system for studying the control of flexible arms. *J. Neurosci.* 16: 7297–7307, 1996.
- HOCHNER, B., PARNAS, H., AND PARNAS, I. Effects of intra-axonal injection of Ca^{2+} buffers on evoked release and on facilitation in the crayfish neuromuscular junction. *Neurosci. Lett.* 125: 215–218, 1991.
- HOYLE, G. (Editor). *Identified Neurons and Behavior of Arthropods*. New York: Plenum Press, 1977.
- KEHOE, J. AND MCINTOSH, J. M. Two distinct nicotinic receptors, one pharmacologically similar to the vertebrate $\alpha 7$ -containing receptor, mediate Cl currents in *Aplysia* neurons. *J. Neurosci.* 18: 8198–8213, 1998.
- KIER, W. M. The musculature of squid arms and tentacles: ultrastructure evidence for functional differences. *J. Morphol.* 185: 223–239, 1985.
- KIER, W. M. The arrangement and function of molluscan muscle. In: *The Mollusca, Molluscan Form and Function*, edited by E. R. Trueman and M. R. Clarke; K. M. Wilburg, editor in chief. New York: Academic Press, 1988, vol. 11, p. 211–252.
- KIER, W. M. The fin musculature of cuttlefish and squid (Mollusca, Cephalopoda): morphology and mechanics. *J. Zool. (Lond.)* 217: 23–38, 1989.
- KIER, W. M., AND SMITH, K. K. Tongues, tentacles and trunks: the biomechanics of movement in muscular-hydrostats. *Zool. J. Linn. Soc.* 83: 307–324, 1985.
- KIER, W. M., SMITH, K. K., AND MIYAN, J. A. Electromyography of the fin musculature of the cuttlefish *Sepia officinalis*. *J. Exp. Biol.* 143: 17–31, 1989.
- KOZAK, J. A., WEIS, K. R., AND BREZINA, V. Two ion currents activated by acetylcholine in the ARC muscle of *Aplysia*. *J. Neurophysiol.* 75: 660–677, 1996.
- LAURIENTI, P. J. AND BLANKENSHIP, J. E. Parapodial swim muscle in *Aplysia brasiliana*. I. Voltage-gated membrane currents in isolated muscle fibers. *J. Neurophysiol.* 76: 1517–1530, 1996.
- LAURIENTI, P. J. AND BLANKENSHIP, J. E. Properties of cholinergic responses in isolated parapodial muscle fibers of *Aplysia*. *J. Neurophysiol.* 82: 778–786, 1999.
- MANABE, T., RENNER, P., AND NICOLL, R. A. Postsynaptic contribution to long-term potentiation revealed by the analysis of miniature synaptic currents. *Nature* 355: 50–55, 1992.
- MANLY, B.F.J. *Randomization, Bootstrap and Monte Carlo Methods in Biology*. London: Chapman and Hall, 1997.
- MARTOJA, R. AND MAY, R. M. Comparison de l'innervation brachiale des Céphalopodes *Octopus vulgaris* Lam. et *Sepiola rondeleti* Leach. *Archs. Zool. Exp. Gén.* 94: 1–60, 1956.
- MARTY, A. AND NEHER, E. Tight-seal whole-cell recording. In: *Single-Channel Recording*, edited by B. Sakmann and E. Neher. New York: Plenum Press, 1995, p. 31–51.
- MCPHERSON, D. R. AND BLANKENSHIP, J. E. Neural control of swimming in *Aplysia brasiliana*. I. Innervation of parapodial muscle by pedal ganglion motoneurons. *J. Neurophysiol.* 66: 1338–1351, 1991.
- MOCHIDA, S., YOKOYAMA, C. T., KIM, D. K., ITOH, K., AND CATTERALL, W. A. Evidence for a voltage-dependent enhancement of neurotransmitter release mediated via the synaptic protein interaction site of N-type Ca^{2+} channels. *Proc. Nat. Acad. Sci. USA* 95: 14523–14528, 1998.
- PACKARD, A. Organization of cephalopod chromatophore system: a neuromuscular image-generator. In: *Cephalopod Neurobiology*, edited by N. J. Abbot, R. Williamson, and L. Maddock. New York: Oxford Science Publications, 1995, p. 331–367.
- PARNAS, H., DUDEL, J., AND PARNAS, I. Neurotransmitter release and its facilitation in crayfish. I. Saturation kinetics of release and of entry and removal of calcium. *Pflügers Arch.* 393: 232–236, 1982.
- PARNAS, H. AND PARNAS, I. Neurotransmitter release at fast synapse. *J. Membr. Biol.* 142: 267–279, 1994.
- PARNAS, I. AND ATWOOD, H. L. Phasic and tonic neuromuscular systems in the abdominal extensor muscles of the crayfish and rock lobster. *Comp. Biochem. Physiol.* 18: 701–723, 1966.
- RALL, W. Theoretical significance of dendritic trees for neuronal input-output relations. In: *Neural Theory and Modeling*, edited by R. Reiss. Stanford, CA: Stanford Univ. Press, 1964, p. 73–97.
- RALL, W. Time constants and electrotonic length of membrane cylinders and neurons. *Biophys. J.* 9: 1483–1508, 1969.
- RINZEL, J. AND RALL, W. Transient response in a dendritic neuron model for current injected at one branch. *Biophys. J.* 14: 759–790, 1974.
- ROGERS, C. M., NELSON, L., MILLIGAN, B. J., AND BROWN, E. R. Different excitation-contraction coupling mechanisms exist in squid, cuttlefish and octopod mantle muscle. *J. Exp. Biol.* 200: 3033–3041, 1997.
- SHIMONI, Y., ALNAES, E., AND RAHAMIMOFF, R. Is hyperosmotic neurosecretion from motor nerve endings a calcium-dependent process? *Nature* 267: 170–172, 1977.
- STOCKBRIDGE, N. AND STOCKBRIDGE, L. L. Properties of synaptic transmission at the neuromuscular junction of the squid, *Loligo opalescence*. *J. Comp. Biochem. Physiol.* 91: 557–564, 1988.
- TAKEUCHI, A. AND TAKEUCHI, N. On the permeability of end-plate membrane during the action of transmitter. *J. Physiol. (Lond.)* 154: 52–67, 1960.
- VAN DER KLOOT, W. The regulation of quantal size. *Prog. Neurobiol.* 36: 93–130, 1991.
- WILSON, D. M. Nervous control of movement in cephalopods. *J. Exp. Biol.* 37: 57–72, 1960.
- YOUNG, J. Z. The diameters of the fibres of the peripheral nerves of *Octopus*. *Proc. Roy. Soc. B Biol. Sci.* 162: 47–79, 1965.
- ZUCKER, R. S. Short-term synaptic plasticity. *Annu. Rev. Neurosci.* 12: 13–31, 1989.